

Comparison of S Poisoning Effects on CO Adsorption on Pd, Au, and Bimetallic PdAu (111) Surfaces

Li-Yong Gan,^{†,‡} Yu-Xia Zhang,[†] and Yu-Jun Zhao^{*,†,‡}

Department of Physics and School of Material Science and Engineering, South China University of Technology, Guangzhou 510640, P. R. China

Received: June 25, 2009; Revised Manuscript Received: December 4, 2009

S and CO adsorption and coadsorption on Pd(111), Au(111), and PdAu(111) surfaces were studied, with the aim of providing insight into the poisoning effects of S and searching for novel sulfur-tolerant catalyst materials by first-principles calculations. It was found that both neighboring and next-nearest-neighboring adsorption sites are poisoned by a single preadsorbed S atom for CO adsorption on Pd(111). On Au(111), E_{ad} of CO increases because of preadsorbed S, indicating that preadsorbed sulfur does not always act as a poison. The bimetallic PdAu(111) surface was found to have better S poison resistance than the Pd(111) and better activity than the Au(111) monometallic surfaces for CO adsorption. Meanwhile, the CO stretching frequencies on each surface with and without S were calculated to depict the effects of S preadsorption on the C–O bond strength.

1. Introduction

Sulfur is well-known for its poisoning effects on many heterogeneous catalytic reactions. It has been reported that even a small amount of S-containing species (often found as impurities in petroleum-derived chemical feed stocks and synthesis gas and automobile exhaust gas) has remarkably negative effects on the performance of the catalysts used in such reactions, such as Pd catalysts and Pd-based membranes.^{1,2} This can cause deactivation of these materials after long-term operation. Uncontrolled and accidental poisoning by S can be a considerable financial burden in the petrochemical and automobile industries.³ To trace the roles of the poisons in heterogeneous catalytic processes, many experimental and theoretical studies have been carried out over several decades. Early studies^{4–6} held that poisoning by an electronegative atom such as S is caused by its accepting charge from the surface that would otherwise contribute to a rate-limiting reaction step. This theory implies that the higher the electronegativity of an adsorbate is, the more conspicuous the poisoning effect should be. Through theoretical calculations on the electronic structure perturbations induced by S on Rh(001), Feibelman et al.⁷ suggested the local density of states (LDOS) near the Fermi level, which governs the ability of the surface to respond to the presence of other species, is substantially reduced by S even at nonadjacent Rh sites. Therefore, they concluded that an extended electron effect is dominant in catalytic deactivation by S.

Meanwhile, CO oxidation on transition-metal surfaces forms the basis for the catalytic removal of CO from car exhaust gases. CO adsorption is commonly used as a probe to explore the chemical activities of monometallic and alloyed surfaces, especially the changes between native and modified surfaces, including composition and electronic properties, by both experimental and theoretical studies. S and CO coadsorption on Ni(111),⁸ Rh(111),⁹ Ru(100),¹⁰ and Cu(100)¹¹ has been

intensively studied by experiments, which also supported the conclusion of a long-range interaction of S. Conclusively, the S poisoning effect is usually explained by a combination of steric (or structural) effects and electronic effects. The former generally describes S blocking contiguous adsorption sites needed by other species, displaying a short-range effect, whereas the latter is associated with charge redistribution or hybridization (i.e., sp or sd), showing a long-range influence.

S poisoning is inevitable, and S–metal interactions are so strong that it is hard to remove S atoms from metal surfaces. It is urgent to find efficient ways to minimize the negative effects of S poisoning and improve the sulfur resistance of metal catalysts in heterogeneous catalysis. Meanwhile, bimetallic alloys provide a new field for catalyst design because of their greater flexibility in chemical composition and interatomic distances compared to pure metals. In fact, bimetallic catalysts are very interesting and promising because their unique catalytic properties are often superior to those of pure metals.¹² In general, the excellent properties of bimetallic surfaces depend on either electronic effects or ensemble effects or both.¹³ For instance, PdAu bimetallic surfaces, because of their peculiar activity and selectivity to vinyl acetate,^{14,15} have attracted increasing interest recently. Earlier density functional theory (DFT) calculations^{16,17} and experiments^{18,19} demonstrated the extraordinary activity of highly dispersed Pd sites and Pd monomers in contact with Au. The surface configuration of Pd monomers has a substantial effect on the activity and stability. The Au-to-Pd ratio on the surface of the particles can be finely tuned to achieve optimal catalytic performance.¹⁸ On the other hand, Yi et al.²⁰ observed that the surface concentration of Pd is a function of annealing temperature and that the surface Pd concentration remains constant, about 20%, between 700 and 1000 K. They also indicated that the surface composition can be systematically controlled by altering the bulk Pd–Au alloy concentration. An experimental study of the sulfur resistance of bimetallic Pd–Au catalysts was conducted with X-ray diffraction and kinetic data, and indicated that gold addition could improve catalyst resistance to sulfur poisoning.²¹ Furthermore, the chemisorption properties of CO on top of a Pd monomer were found to be little affected

* Corresponding author. Tel.: +86-20-87110426. Fax: +86-20-87112837. E-mail: zhaojy@scut.edu.cn.

[†] Department of Physics.

[‡] School of Material Science and Engineering.

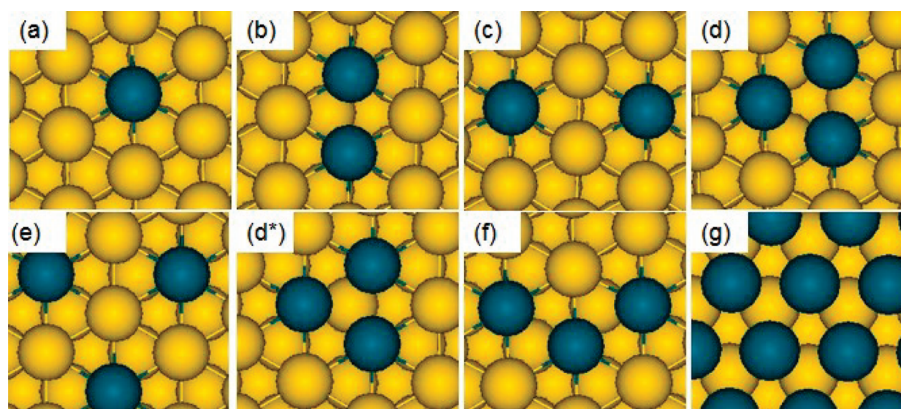


Figure 1. Configurations of PdAu(111) surfaces studied in this work. In each ensemble, Pd atoms substitute for Au atoms on the topmost layer. The yellow and blue balls represent Au and Pd atoms, respectively.

by other CO molecules on top of second-neighbor Pd monomers.²² From a theoretical point of view, there have been few studies on the effect of S poisoning on Pd–Au surfaces.

In this work, we have performed DFT calculations to compare S and CO adsorption and coadsorption on Pd(111), Au(111), and PdAu(111), in order to shed some light on S poisoning effects and the activity of bimetallic PdAu(111), as well as to promote the search for novel catalytic materials with high sulfur tolerance.

2. Computational Details

This work was conducted with the Vienna Ab Initio Simulation Package (VASP)^{23–26} with the frozen-core projector-augmented-wave (PAW) method.^{27,28} The Perdew–Wang (PW91) generalized gradient approximation (GGA)^{29,30} functional was employed for the exchange-correlation energy. Both monometallic and bimetallic surfaces were modeled with a five-layer slab with a vacuum thickness of 15 Å. The adsorbed species were put on one side of the slab. The three uppermost layers were fully relaxed, whereas the two bottommost layers were fixed at their bulk structure. A cutoff energy of 500 eV was employed in this work. A 3 × 3 supercell was used to simulate sulfur and CO adsorption and coadsorption on monometallic and bimetallic surfaces, and a 4 × 4 supercell was used to describe the relative stability of a series of bimetallic PdAu(111) surfaces (Figure 1). We employed Monkhorst–Pack k -point grids of 5 × 5 × 1 and 3 × 3 × 1 for the 3 × 3 and 4 × 4 surface unit cells, respectively. The lattice constant of Pd bulk was fully optimized to 3.96 Å, within an error of 2% in comparison with the experimental value of 3.89 Å.³¹ The lattice constant of bulk Au was determined to be 4.18 Å, within ~2.5% deviation from experimental value (4.08 Å). For the bimetallic PdAu(111) surfaces, the lattice constant of bulk Au was adopted, because a relative low concentration of Pd in the surface was assumed in the present study.

The adsorption energies of S and CO on monometallic and bimetallic surfaces in this work were calculated as

$$E_{\text{ad}} = -(E_{\text{A/M}} - E_{\text{M}} - E_{\text{A}}) \quad (1)$$

where $E_{\text{A/M}}$ is the total energy of the respective adatom/molecule adsorbed on the metal surface, E_{M} is the total energy of the clean metal surface, and E_{A} is the total energy of the adatom/molecule in the gas phase. M in eq 1 denotes the metal surfaces Pd(111), Au(111), and PdAu(111).

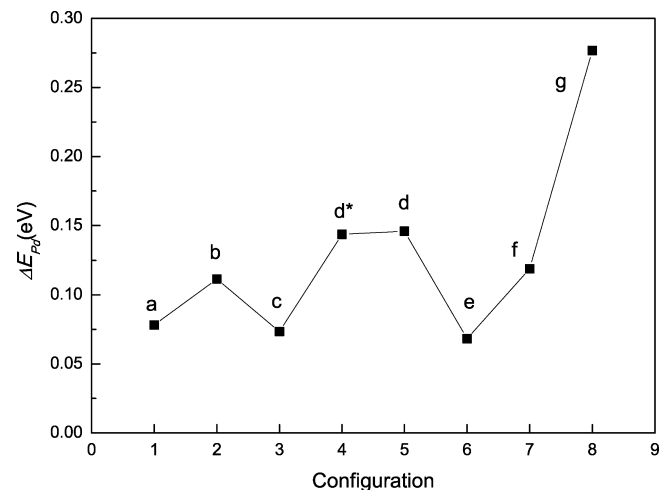


Figure 2. Formation energies of various PdAu(111) bimetallic surfaces defined by eq 2. Labels a–g correspond to the configurations shown in Figure 1.

3. Results and Discussions

3.1. Stability of PdAu(111) Bimetallic Surface. 3.1.1. Formation Energy. First, we tested the energetic stability of the bimetallic PdAu(111) configurations shown in Figure 1, in which each ensemble had a different number of Pd atoms and the formation energies of each configuration were given by¹⁶

$$\Delta E_{\text{Pd}} = [E_{\text{PdAu}} - E_{\text{Au surf}} + N_{\text{Pd}}(\mu_{\text{Au}} - \mu_{\text{Pd}})]/N_{\text{Pd}} \quad (2)$$

Here, E_{PdAu} and $E_{\text{Au surf}}$ represent the total energies of the PdAu(111) surface and clean Au(111) slab, respectively. μ_{Au} and μ_{Pd} are the atom chemical potentials of Au and Pd, respectively, and were both determined to be in equilibrium with their respective bulk reservoir. N_{Pd} is the number of Pd atoms in the unit cell. The change in the total energy was normalized by the number of Pd atoms to allow comparison between ensembles with different numbers of Pd substitutions. The calculated results are depicted in Figure 2.

It is obvious that ensembles with first-neighbor Pd pairs (Figure 1b,d,d*,f,g) are energetically unfavorable compared to ensembles with noncontiguous Pd pairs (Figure 1a,c,e). This is in good agreement with previous theoretical¹⁶ and experimental^{18,20} studies. In those works, the most prevalent surface ensemble was found to consist of Pd monomer sites surrounded by Au. This might result from the fact that the Pd–Au bond is slightly

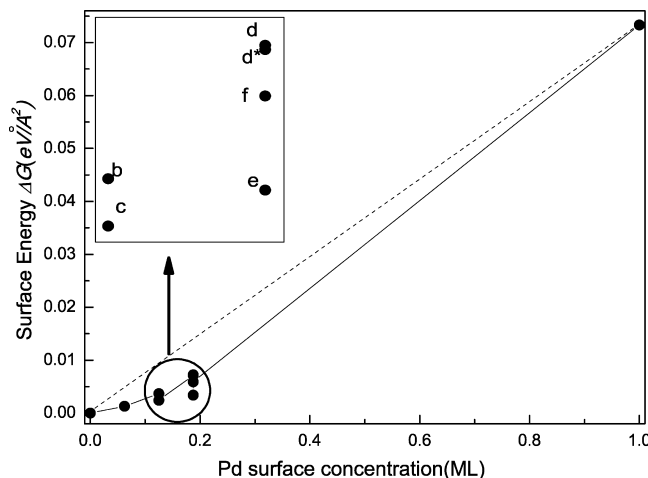


Figure 3. Changes in Gibbs surface energy (cf. eq 3) as a function of Pd concentration on the Au(111) surface. The energy zero corresponds to the surface energy of the clean Au(111) surface. The straight dashed line was obtained by joining the points representing pure Au and a Pd monolayer. The circled region is enlarged in the inset.

ionic and stronger than the Pd–Pd and Au–Au bonds,¹⁶ and hence, as many Pd–Au bonds are formed as possible. As a result, the favorable Pd–Au structure might avoid the formation of bulk Pd₄S,²¹ which is a main source of S poisoning.³²

3.1.2. Surface Free Energy. To further investigate the stability properties of PdAu(111) surface, we investigated the change in Gibbs free energy caused by exchanging a Pd atom with the surface, which is defined³³ as

$$\Delta G = (G_{\text{PdAu}} - G_{\text{slab}} - \Delta N_{\text{Au}} \mu_{\text{Au}} - N_{\text{Pd}} \mu_{\text{Pd}})/A \quad (3)$$

Here, G_{PdAu} is the free energy of the PdAu surface, G_{slab} is the free energy of the Au slab, ΔN_{Au} is the difference in the number of Au atoms between the bimetallic system and the clean slab, and N_{Pd} is the number of Pd atoms in the surface. The chemical potentials of Au and Pd were still treated as being in equilibrium with their bulk reservoirs. The change in Gibbs free energy was normalized by the surface area A for comparison between various configurations with different unit cell. This definition is also called the “surface free energy”. Here, we note that the effects of temperature and pressure are not taken into account. Consequently, the free energies G_{PdAu} and G_{slab} are identical to the calculated total energies of E_{PdAu} and E_{slab} .

The results are shown in Figure 3. The positive slope of the Gibbs free energy change of PdAu as a function of Pd concentration curve implies that it is energetically unfavorable for Pd impurities to migrate to the surface rather than staying in the bulk, consistent with the fact that the surface energy of Pd (2.043 J/m^2)³⁴ is higher than that of Au (1.626 J/m^2).³⁵ Thus, the PdAu(111) surface will not be dominated by Pd atoms at temperatures below 1000 K, as reported by Yi et al.²⁰ On the other hand, the curve is slightly convex, indicating that noncontiguous Pd pairs are more preferable in the surface. Meanwhile, from the inset in Figure 3, one can see that, at the same Pd concentration (i.e., for configurations b and c, as well as for configurations d, d*, e, and f), noncontiguous Pd pairs are more favored. Thus, from this aspect, it can also be deduced that the Pd atoms will form a Pd–Au alloy rather than aggregate into larger particles.

3.2. Adsorption of S and CO on Metal Surfaces.

3.2.1. Pure Metal (Pd, Au) Surfaces. Before S and CO adsorption on PdAu(111) was studied, their adsorptions on

TABLE 1: Adsorption Energies (eV) and Structural Parameters^a

	E_{ad} of S (eV)	$d_{S-\text{M}}^b$ (Å)	E_{ad} of CO (eV)	$d_{\text{Surf-C}}^c$ (Å)	$d_{\text{C-O}}^d$ (Å)
Pd(111)					
top	4.08	2.15	1.43	1.87	1.16
bridge	—	—	1.84	1.41	1.18
fcc	5.96	2.25	2.04	1.28	1.17
hcp	5.89	2.25	2.02	1.28	1.20
Au(111)					
top	3.03	2.27	0.19	2.04	1.15
bridge	—	—	0.17	1.46	1.17
fcc	4.47	2.41	0.13	1.32	1.18
hcp	4.32	2.42	0.15	1.36	1.18

^a The maximum adsorption energy is emphasized in bold for each system. ^b S–metal bond length. ^c Height of CO above each metal surface. ^d C–O bond length.

monometallic Pd(111) and Au(111) surfaces were calculated, and the results are listed in Table 1. It is obvious that the most preferred sites for S on both Pd(111) and Au(111) surfaces are face-centered cubic (fcc). The bridge site is unstable, because the adsorbed S atom would relax spontaneously to the nearby fcc sites. The calculated S–Pd and S–Au bond lengths of the energetically favored structure are 2.25 and 2.41 Å, respectively. The most favorable sites for CO adsorption on Pd(111) and Au(111) are fcc and top sites, with adsorption energies of 2.04 and 0.19 eV, respectively. The heights of the CO molecule above the Pd(111) and Au(111) surfaces ($d_{\text{S-C}}$) are 1.28 and 2.04 Å, respectively, at the favored site on each surface, and the corresponding C–O bond distances ($d_{\text{C-O}}$) at these sites are 1.17 and 1.15 Å (see Table 1). These results are in good agreement with previous experimental^{36–40} and theoretical^{16,41–44} studies.

According to the d-band center theory, the closer the d-band center (ε_d)⁴⁵ is to the Fermi level, the easier the charge transfer between the metal surface and adsorbates. Here, we employ the d-band center as an initial measurement to investigate the poisoning effects of S on Pd(111) and Au(111). Meanwhile, the density of states (DOS) near the Fermi level can also reflect the activity of metal surfaces to a certain extent.⁷ We also calculate the DOS at the Fermi level of the metal surfaces to weigh the influence of sulfur on the metal chemical activity from another perspective. The results calculated for the d-band center (ε_d) and DOS at the Fermi level are listed in Table 2.

For the Pd(111) surface, it was found that the ε_d value of the first-nearest Pd atom of S is lowered to -2.51 from -1.87 eV for the clean surface. This suggests that the activities of the nearest hcp sites h1 and the next neighboring fcc sites f1 (shown in Figure 4a) are strongly affected. Previous DFT and experimental studies have reported that the adsorption of S would induce a large decrease in the DOS of metal d states near the Fermi level on a series of transition-metal surfaces.^{46–49} In this work, all three nonequivalent types of Pd atoms (shown in Figure 4a) experienced a distinct decrease of d states at the Fermi level when S was adsorbed, especially the three nearest Pd atoms of type 1. One can conclude that the poisoning effects of S on the Pd(111) surface might be a fairly long-range effect that would significantly affect the adsorption of other adsorbates such as CO, weaken the interaction between the Pd surface and CO, and ultimately affect the reaction rate. This can be confirmed from the partial density of states (PDOS) plots of the Pd–S system in Figure 5a. A distinct overlapping between S p and Pd d states on pure Pd(111) could be found around -5.2 eV, suggesting a strong covalent bond between S and the Pd

TABLE 2: S-Induced Electronic Structural Changes on Pd(111) and Au(111) Surfaces

system	ε_d (eV)				DOS at E_f (states/eV)				charge on S (e^-) ^b
	clean ^a	1	2	3	clean ^a	1	2	3	
Pd-S-fcc	-1.87	-2.51	-1.86	-1.92	1.919	1.047	1.812	1.832	6.230
Au-S-fcc	-3.38	-3.68	-3.41	-3.41	0.098	0.214	0.113	0.133	6.357

^a Indicating clean surface without S. ^b From Bader population analysis.⁵²

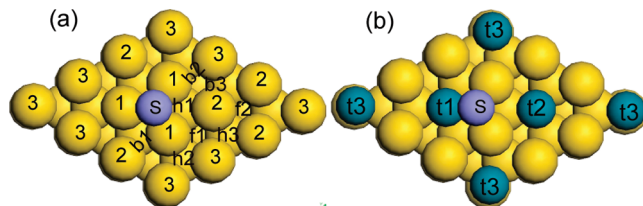


Figure 4. Possible CO adsorption sites on S-preadsorbed metal surfaces. (a) S-preadsorbed monometallic Pd(111) or Au(111), where the first-, second-, and third-nearest-neighbor metal atoms relative to the adatom S are labeled 1, 2, and 3, respectively. The letters b, f, and h represent the bridge, hcp, and fcc sites, respectively, while the top sites are simply indicated by 1, 2, or 3. (b) S-preadsorbed PdAu(111) surface. The top sites of Pd atoms are indicated by t1, t2, and t3. The yellow and aqua balls denote Au and Pd atoms, respectively. The first-, second-, and third-nearest-neighbor Pd atoms relative to S are indicated by 1, 2, and 3, respectively.

substrate. The rehybridization features are not restricted to the first-nearest Pd atom, but extend to the second- and third-nearest Pd atoms (see the arrows in Figure 5a). However, for the Au(111) surface, the downward shift of ε_d is not as evident as for the Pd(111), being 0.3 vs 0.64 eV. Interestingly, the partial densities of states of the Au d states at the Fermi level of the three nonequivalent Au atoms are increased because of the adsorbed S atom, especially that of the first-nearest Au atom. This suggests that S might increase the activity of the Au(111) surface. In Figure 5b, there are two main peaks in the S p curve, and the higher one below the Fermi level (antibonding state) is partially filled. Therefore, S binding to Au(111) is much weaker than S binding to Pd(111). From a Bader charge analysis, it is clear that charge is transferred from the metal surface to the S atom.

3.2.2. PdAu(111) Surfaces. From the results discussed in section 3.1, we model the PdAu(111) surface with noncontiguous Pd pairs homogeneously distributed in the surface layer and each Pd atom surrounded by six Au atoms for S and CO adsorption (Figure 6). We use the tt, bb, ff, and hh followed by numbers to represent adsorption sites for each adsorbate (S and CO) on this well-defined PdAu(111) surface. The results are listed in Table 3. For S adsorption, the most preferred site is ff1 with one Pd and two Au atoms surrounding it. The two types of bridge sites and the top site on Au are energetically unstable, as the S atom would relax spontaneously to a nearby hollow site (hh1 or ff1). For CO adsorption, the most energetically favorable site is on top of a Pd atom, namely, tt1 (shown in Figure 6), in good agreement with Mazzzone et al.'s study.²²

To compare the results for PdAu(111) with those for the two parent metal surfaces, adsorption energies of CO and S on PdAu(111) with respect to those of S and CO on Pd(111) and Au(111) are plotted in Figure 7. It is noted that S adsorption is significantly stronger than CO adsorption on these three metal surfaces. From Pd(111) to PdAu(111), the E_{ad} value of S decreases markedly, and the change is much greater than that for CO, indicating that the effect of the bimetallic surface on S is more notable than that on CO. On the other hand, on top of the Pd atoms of PdAu(111), E_{ad} for CO is very close to the

value for the top site on pure Pd(111). These phenomena suggest that PdAu(111) might be less likely to be poisoned by S-containing impurities in reactants. Typically, if the binding energy is too high, the adsorbates will not desorb easily from the surface; i.e., they will block the site and affect further adsorption of other adsorbates, such as CO on Pt clusters.⁵⁰ Even if the surface is poisoned, S should be much easier to remove from the PdAu(111) surface. The weaker bonding for S on the PdAu(111) surface might originate from the configuration discussed in section 3.1. However, from Au(111) to PdAu(111), the adsorption energies of CO increase much more markedly, although the adsorption energies of S also increase. The increment of E_{ad} for CO is almost 3 times greater than that for S. This means that the bimetallic PdAu(111) surface is more active than the Au(111) surface, but at the same time, it retains the low activity toward S of the Au(111) surface. The bimetallic PdAu(111) surface might be more S-resistant than Pd(111) and more active than Au(111), and thus, the catalytic performance of the bimetallic PdAu(111) surface might be better than those of the two parent surfaces, Pd(111) and Au(111).

3.3. Coadsorption of S and CO on Metal Surfaces. The coadsorption was modeled with S preadsorbed at the middle fcc hollow site on all three metal surfaces with CO at various trial fcc and hcp sites on Pd(111), top and bridge sites on Au(111), and top sites on Pd atoms on PdAu(111), as shown in Figure 4. The coadsorption energy of CO on S-preadsorbed metal surfaces is defined as

$$E_{ad} = -(E_{CO/S-M} - E_{S/M} - E_{CO}) \quad (4)$$

where $E_{CO/S-M}$, $E_{S/M}$, and E_{CO} are the energies of CO and S coadsorbed on a metal surface, the S-preadsorbed metal surface, and a CO molecule in the gas phase, respectively. The results are listed in Table 4. It was found that CO is somewhat tilted (with the C atom close to S and the O atom away from S) as it gets close to S on the three metal surfaces. For instance, the O—C—Au angle is 175° at t2 and 127.5° at t1 on S-preadsorbed Au(111), and the O—C—Pd angle is 165.4° at t1 on S-preadsorbed PdAu(111). This behavior should be attributed mainly to the electrostatic interaction between the S monopole (negative) and the CO dipole. The tilted angle of the CO molecule with respect to the metal surface becomes smaller as the distance between CO and the S atom increases. The C—M and C—O bond lengths do not appear to change in the coadsorption system relative to those on pure metal surfaces.

On the S-preadsorbed Pd(111) surface, CO adsorption at all of the studied sites was weakened, with the first-nearest hcp hollow sites (h1) being especially unstable. CO at these sites would relax spontaneously to the nearby t2 sites because of the strong repulsion between the two adsorbates. This indicates that the presence of the S atom would directly block nearby CO adsorption sites. Accordingly, E_{ad} of CO at the next-nearest hollow sites, three hcp (h2) and six fcc (f1) sites, is decreased markedly compared to E_{ad} of CO on clean Pd(111). Furthermore, the third-nearest hollow sites h3 and f2 are also affected more

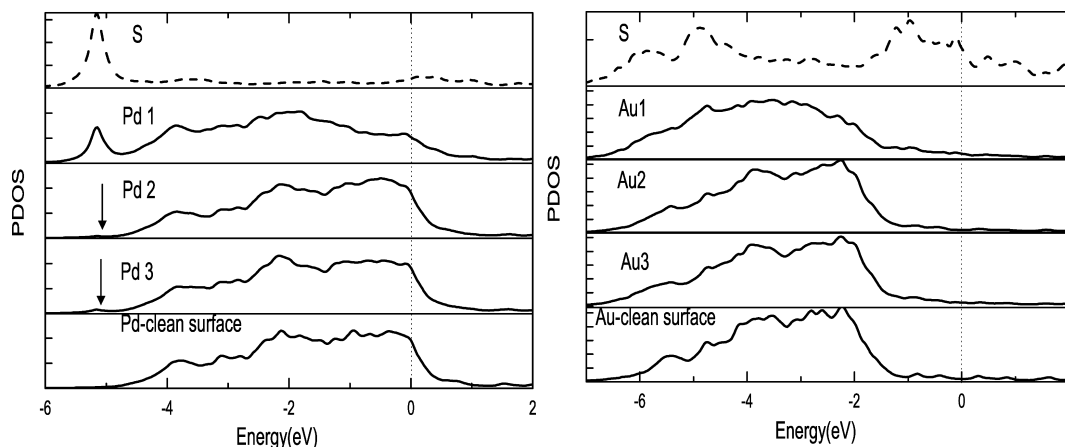


Figure 5. PDOS ($E_{\text{Fermi}} = 0$) for S on M(111) for (a) Pd(111) and (b) Au(111). Solid lines, M d states; dashed lines, S p states on each M(111) surface. The adatom S and the three nonequivalent metal surface atoms are illustrated in Figure 4a. PDOS of d states for the two clean metal surfaces are also shown.

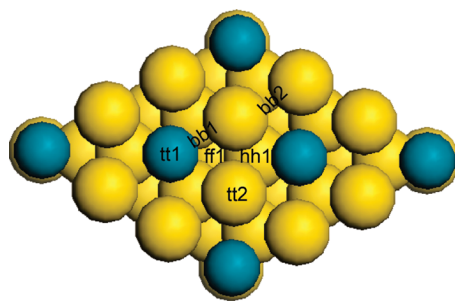


Figure 6. Diagram of adsorption sites for S and CO on the PdAu(111) surface. Yellow and aqua balls represent surface-layer Au and Pd atoms, respectively. Double-letter notations are used to distinguish the CO adsorption sites from those in Figure 4: tt1 and tt2, on top of a Pd atom and a Au atom, respectively; bb1, between one Pd atom and one Au atom; bb2, between two Au atoms; ff1 and hh1, fcc and hcp sites, respectively, surrounded by one Pd and two Au atoms.

TABLE 3: Adsorption Energies (eV) for S and CO on PdAu(111) for the Adsorption Sites Shown in Figure 6

	tt1	tt2	bb1	bb2	ff1	hh1
E_{ad} of CO (eV)	1.18	0.42	0.96	—	0.90	0.91
E_{ad} of S (eV)	3.30	—	—	—	4.82	4.61

or less, with CO coadsorption energies of 1.95 and 2.00 eV, respectively. This confirms that the effect of S on Pd(111) could extend to the third-nearest hollow sites. These results are in line with previous experimental observations.^{11,51} In ref 11, the spatial extent of the interaction between S and CO on Cu(100) surface was deduced to elucidate the effective range of S poisoning effects, and the extent was found to contain all first- and second-nearest Cu atoms and some third-nearest Cu atoms.

It is common that adsorption would be weakened when coverage is increased, and the presence of S would usually hinder the adsorption of other adsorbates [such as the above-discussed S and CO coadsorption on Pd(111)]. For the S-preadsorbed Au(111) surface, however, we obtained an unexpected result. The adsorption of CO was found to be enhanced at all sites on S-preadsorbed Au(111), except b2 (shown in Figure 4). First, the adsorption of CO at the first-nearest sites t1 and b1 was unstable, and that at b2 was weakened. This might be because of the natural repulsion between S and CO. When CO was a little farther from S, for example, at t2 or b2, the E_{ad} value of CO was markedly increased. When the distance between S and CO was even longer, at t3, the E_{ad} value of CO decreased, but was still higher than that on the clean Au(111)

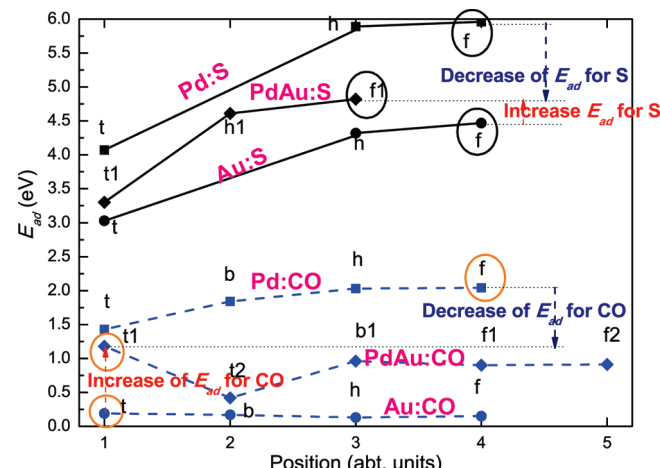


Figure 7. Comparison of E_{ad} values of S and CO on Pd(111), Au(111), and PdAu(111) surfaces (Figure 6). Black solid and green dashed lines represent adsorption of S and CO, respectively. Squares, triangles, and diamonds stand for adsorption on Pd(111), Au(111), and PdAu(111), respectively. Circles indicate the most energetically preferred sites for CO/S on the three metal surfaces.

TABLE 4: Adsorption Energies (eV) of CO on S-Ppreadsorbed Pd(111), Au(111), and PdAu(111) at Various Sites, Shown in Figure 4

on Pd (111)	E_{ad} of CO (eV)	on Au (111)	E_{ad} of CO (eV)	on PdAu (111)	E_{ad} of CO (eV)
h1	—	t1	—	t1	0.54
h2	1.76	t2	0.29	t2	1.06
h3	1.95	t3	0.25	t3	1.11
f1	1.68	b1	—		
f2	2.00	b2	0.09	b3	0.40

surface. Analogous results were reported in refs 40 and 52. In ref 40, Xue et al. found that the activation energy of water dissociation decreased sharply on sulfur-preadsorbed Au(111). In ref 52, Zhang et al. also found that the adsorption energy of CO increased on the NO_2^- , S-, O-, or Cl-preadsorbed Au(111) surface. The increased adsorption energy of CO on the NO_2^- -preadsorbed Au(111) surface was explained by the attractive dipole interaction between CO and NO_2^- , which is not appropriate for illustrating the phenomenon of S (or O or Cl) and CO coadsorption on Au(111). Obviously, S might behave as a poison no more on Au(111) than on other catalyst surfaces, but it will act as an activator in some cases, although the detailed

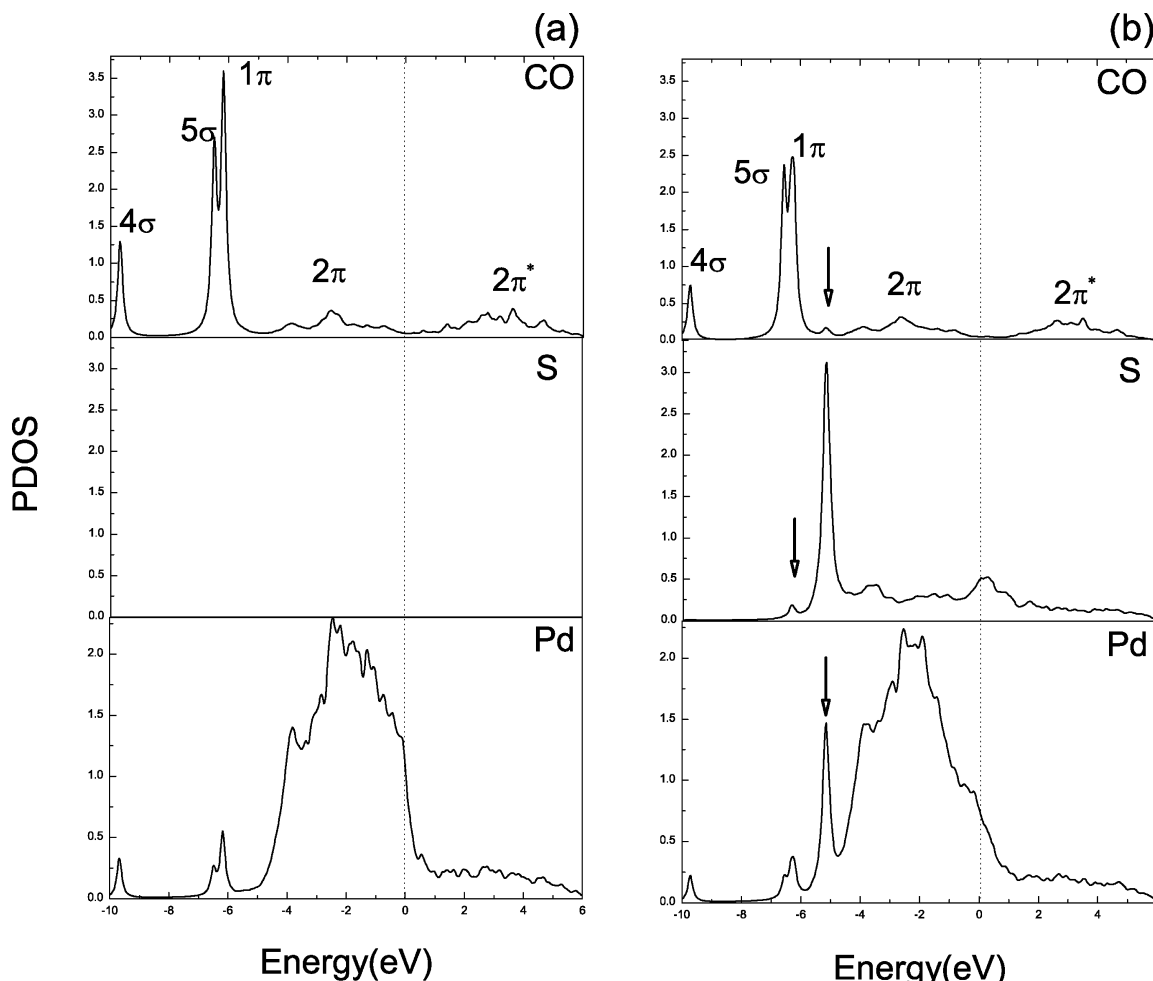


Figure 8. PDOS of CO adsorption on Pd(111) surfaces (a) with and (b) without S. Part b corresponds to the configuration of CO at an f1 site on S-preadsorbed Pd(111) (shown in Figure 4).

mechanism is not clear. If these unusual phenomena of S were clearly understood, this might provide some new approaches to improve the catalytic performance of Au-based catalysts.

Figure 8 presents a PDOS comparison between CO adsorption on Pd(111) surfaces with and without S to examine why S poisons CO adsorption at such a long range. Because of the presence of S, there is a marked decrease of the 5σ and 1π peaks on the CO side. Meanwhile, an obvious decrease of the peaks around -6.2 eV overlapping with CO resonance (5σ and 1π) and a noticeable peak at the energy of S-related bonding state at about -5.2 eV were found for Pd d states. In addition, there is a clear contribution of S to the CO–surface interaction around -6.2 eV, and a direct interaction between CO and S could also be found around -5.2 eV (see the arrows in Figure 8b). These features clearly indicate that the CO molecule interacts directly with the S adatom. We conclude that the marked decrease of E_{ad} of CO on S-preadsorbed Pd(111) relative to clean Pd(111) might be caused by spatially localized S–Pd bonding at about -5.2 eV, as well as a direct CO–S interaction.

PDOS plots for CO adsorption on Au(111) surfaces with and without S are shown in Figure 9 in order to gain insight into why a S adatom might improve CO adsorption on Au(111). However, no marked changes in the PDOS can be seen in the plot. In ref 41, Xue et al. expected that the promotion might result from strong electron transfer to the Au(111) surface from the S atom. Nevertheless, we found that, on Au(111), S still behaves as a charge acceptor from a Bader population analysis⁵³ (shown in Table 2). However, the DOS at the Fermi level of

the Au d states increases as S is adsorbed on Au(111), which is different from the typical observation on other transition-metal surfaces^{46–49} and might be responsible for the enhancement of CO adsorption.

For CO on S-preadsorbed PdAu(111), the E_{ad} value of CO is sharply reduced at the t1 site, which is on top of the first-nearest Pd atom relative to the sulfur atom. However, at t2, the decrease of the CO adsorption energy is not remarkable, being 1.05 vs 1.18 eV on clean PdAu(111), suggesting that the influence of the S adatom drops dramatically beyond the adjacent atoms on the PdAu(111) surface. The CO stretching frequencies on each surface with and without S were calculated to depict the effect of S on the C–O bond strength, as reported in Table 5. From Table 5, it is evident that the CO stretching frequencies on the three S-precovered metal surfaces are all blue-shifted with respect to those on the clean metal surfaces. According to the Blyholder model,⁵⁴ the electron back-donation from the metal substrate might decrease because of the presence of the sulfur atom. This brings about a decrease in the occupation of the 2π* antibonding, relative to that on clean surfaces, and results in a blue shift. Meanwhile, the unexpected enhancement of CO adsorption on the Au surface due to electronegative species (such as S) remains unexplained will require further experiments and theoretical analysis.

Finally, the adsorption energy difference of CO on Pd(111) and PdAu(111) surfaces was compared with that on the corresponding S-preadsorbed surfaces, as shown in Figure 10. Apparently, the effective range of S on PdAu(111) is shorter

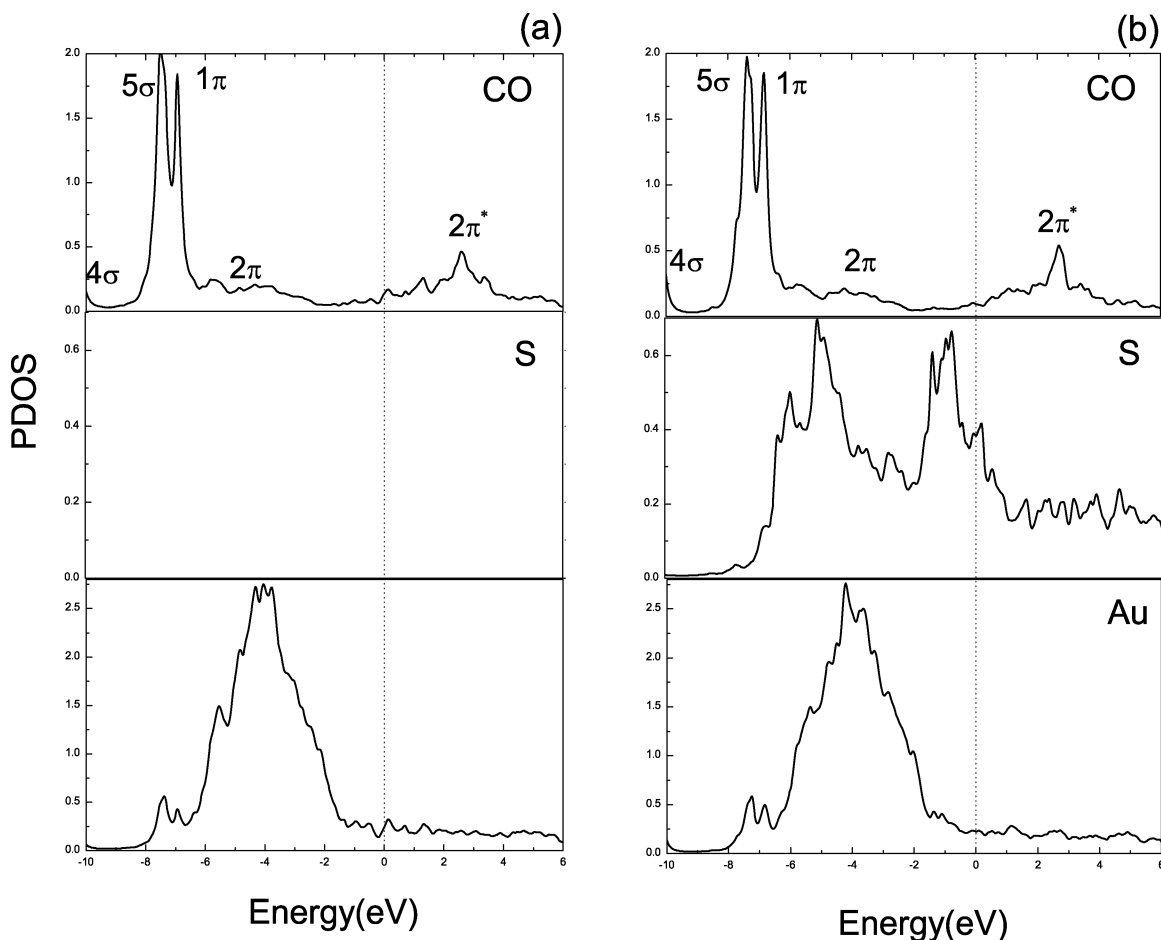


Figure 9. PDOS of CO adsorption on Pd(111) surfaces (a) with and (b) without S. Part b corresponds to the configuration of CO at a b3 site on S-preadsorbed Au(111) (shown in Figure 4).

TABLE 5: Stretching Frequencies, f (cm $^{-1}$), of CO on Each Surface^a

system	site	f (cm $^{-1}$)
gas phase		2139 [2143 ^b]
		1760
Pd(111)	fcc	1776
	hcp	1776
Au(111)	atop	2053
	bridge	1894
PdAu(111)	tt1	2040
	tt2	2068
Pd-S	bb1	1928
	ff1	1848
Au-S	hh1	1883
	f1	1776
PdAu-S	f2	1779
	h2	1771
	h3	1773
	t2	2088
	t3	2064
	b2	1954
	b3	1896
	t1	2035
	t2	2047
	t3	2068

^a Experimental gas-phase value listed in brackets. ^b Reference 55.

than that on pure Pd(111), suggesting that PdAu(111) might be more poison-resistant than Pd(111). Pd atoms in PdAu(111) can be regarded as impurities in the Au(111) surface, which will enhance the localization of their electronic distribution. This might lead to the shorter effective range of S on PdAu(111) with respect to that on Au(111).

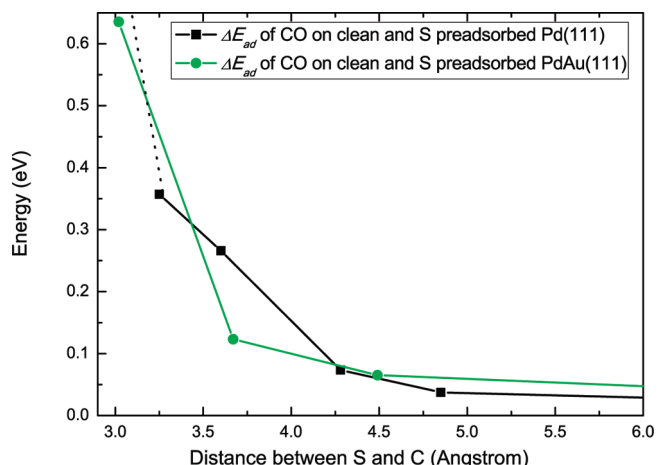


Figure 10. E_{ad} of CO due to the presence of a preadsorbed S atom relative to E_{ad} at the same sites on a clean surface. Black bold and green dashed lines indicate energy differences on Pd(111) and PdAu(111), respectively. The black dotted line depicts the extrapolated value at the nearest-neighbor sites on Pd(111).

4. Summary

The stability of various PdAu(111) bimetallic surfaces was studied systematically by first-principles calculations, along with S and CO adsorption and coadsorption on Pd(111), Au(111), and well-defined PdAu(111) surfaces. We confirmed the structure that the surface of PdAu(111) is enriched in Au and that Pd atoms energetically favor monomer sites surrounded by Au atoms. On Au(111), the presence of S can enhance the

adsorption of CO, suggesting that sulfur does not always act as a poison, but can act as a promoter in some cases. If the detailed mechanism for this effect were clearly known, it could provide new approaches to improve the catalytic performance of Au-based catalysts. From the adsorption energy changes for CO and S on these surfaces, we suggest that the bimetallic PdAu(111) surface might be more poison-resistant than pure Pd(111) and more active than pure Au(111). Additionally, for S-preadsorbed PdAu(111), we found that the effective poisoning range of S was less than that on pure Pd(111). Conclusively, in comparison with the monometallic surfaces, the bimetallic PdAu(111) surface was found to have a better S-poisoning resistance than Pd(111) and have a better activity than Au(111). Frequency calculations showed that the presence of S will induce blue shifts of CO frequencies on all three studied metal surfaces, without any clue as to the reason for the CO adsorption enhancement on Au. Further experiments and theoretical analysis are necessary to explain the unexpected enhancement of CO adsorption on the Au surface due to electronegative species (such as S).

Acknowledgment. We acknowledge the computer time at the High Performance Computer Center of the Shenzhen Institute of Advanced Technology (SIAT), Chinese Academy of Science, and High Performance Grid Computer Center (SCUTGrid) of South China University of Technology. This work was supported by the New Century Excellent Talents Program (Grant NCET-08-0202).

References and Notes

- (1) Lee, J. K.; Rhee, H. K. *J. Catal.* **1998**, *177* (2), 208–216.
- (2) Oudar, J., Wise, H., Eds. *Deactivation and Poisoning of Catalysts*; Marcel Dekker: New York, 1991.
- (3) Rodriguez, J. A.; Hrbek, J. *Acc. Chem. Res.* **1999**, *32* (9), 719–728.
- (4) Kiskinova, M.; Goodman, D. W. *Surf. Sci.* **1981**, *108* (1), 64–76.
- (5) Richter, R.; Wilkins, J. W. *J. Vac. Sci. Technol.* **1983**, *1* (2), 1089–1094.
- (6) Garfunkel, E. L.; Crowell, J. E.; Somorjai, G. A. *J. Phys. Chem. C* **1982**, *86* (3), 310–313.
- (7) Feibelman, P. J.; Hamann, D. R. *Phys. Rev. Lett.* **1984**, *52* (1), 61–64.
- (8) Erley, W.; Wagner, H. *J. Catal.* **1978**, *53* (3), 287–294.
- (9) Goodman, D. W. In *Heterogeneous Catalysis: Proceedings of the Second Symposium of the Industry–University Cooperative Chemistry Program of the Department of Chemistry, Texas A&M University, April 1–4, 1984*; Shapiro, B. L., Ed.; Texas A&M University Press: Austin, TX, 1984; pp 230–251.
- (10) Peden, C. H. F.; Goodman, D. W. In *Proceedings of the Symposium on the Surface Science of Catalysis*; Deviney, M. L., Gland, J. L., Eds.; American Chemical Society: Washington, DC, 1984; pp 185–198.
- (11) Hu, X. F.; Hirschmugl, C. J. *Phys. Rev. B* **2005**, *72*, 205439.
- (12) Rodriguez, J. A. *Prog. Surf. Sci.* **2006**, *81* (4), 141–189.
- (13) Sachtier, W. M. H. *Vide* **1973**, *28* (164), 67–71.
- (14) Han, Y. F.; Wang, J. H.; Kumar, D.; Yan, Z.; Goodman, D. W. *J. Catal.* **2005**, *232* (2), 467–475.
- (15) Chen, M. S.; Kumar, D.; Yi, C. W.; Goodman, D. W. *Science* **2005**, *310* (5746), 291–293.
- (16) Yuan, D. W.; Gong, X. G.; Wu, R. Q. *Phys. Rev. B* **2007**, *75*, 085428.
- (17) Yuan, D. W.; Gong, X. G.; Wu, R. Q. *J. Phys. Chem. C* **2008**, *112* (5), 1539–1543.
- (18) Wang, D.; Villa, A.; Porta, F.; Prati, L.; Su, D. S. *J. Phys. Chem. C* **2008**, *112* (23), 8617–8622.
- (19) Kumar, D.; Chen, M. S.; Goodman, D. W. *Catal. Today* **2007**, *123* (1–4), 77–85.
- (20) Yi, C. W.; Luo, K.; Wei, T.; Goodman, D. W. *J. Phys. Chem. B* **2005**, *109*, 18535–18540.
- (21) Menegazzo, F.; Canton, P.; Pinna, F.; Pernicone, N. *Catal. Commun.* **2008**, *9* (14), 2353–2356.
- (22) Mazzone, G.; Rivalta, I.; Russo, N.; Sicilia, E. *J. Phys. Chem. C* **2008**, *112* (15), 6073–6081.
- (23) Kresse, G.; Hafner, J. *Phys. Rev. B* **1993**, *47* (1), 558–561.
- (24) Kresse, G.; Hafner, J. *Phys. Rev. B* **1993**, *48* (17), 13115–13118.
- (25) Kresse, G.; Furthmüller, J. *Comput. Mater. Sci.* **1996**, *6* (1), 15–50.
- (26) Kresse, G.; Furthmüller, J. *Phys. Rev. B* **1996**, *54* (16), 11169–11186.
- (27) Blöchl, P. E. *Phys. Rev. B* **1994**, *50* (24), 17953.
- (28) Kresse, G.; Joubert, D. *Phys. Rev. B* **1999**, *59* (3), 1758.
- (29) Perdew, J. P.; Yue, W. *Phys. Rev. B* **1986**, *33* (12), 8800.
- (30) Perdew, J. P.; Chevary, J. A.; Vosko, S. H.; Jackson, K. A.; Pederson, M. R.; Singh, D. J.; Fiolhais, C. *Phys. Rev. B* **1992**, *46* (11), 6671.
- (31) Kittel, C. *Introduction to Solid State Physics*, 6th ed.; Wiley: New York, 1986.
- (32) Pernicone, N.; Cerboni, M.; Prelazzi, G.; Pinna, F.; Fagherazzi, G. *Catal. Today* **1998**, *44* (1–4), 129–135.
- (33) Piccinin, S.; Stampfl, C.; Scheffler, M. *Phys. Rev. B* **2008**, *77*, 075426.
- (34) Mezey, L. Z.; Giber, J. *Jpn. J. Appl. Phys. Part 1* **1982**, *21* (11), 1569–1571.
- (35) Anton, R.; Eggers, H.; Veletas, J. *Thin Solid Films* **1993**, *226* (1), 39–47.
- (36) Maca, F.; Scheffler, M.; Berndt, W. *Surf. Sci.* **1985**, *160* (2), 467–474.
- (37) Grillo, M. E.; Stampfl, C.; Berndt, W. *Surf. Sci.* **1994**, *317* (1–2), 84–98.
- (38) Dhanak, V. R.; Shard, A. G.; Cowie, B. C. C.; Santoni, A. *Surf. Sci.* **1998**, *410* (2–3), 321–329.
- (39) Giessel, T.; Schaff, O.; Hirschmugl, C. J.; Fernandez, V.; Schindler, K. M.; Theobald, A.; Bao, S.; Lindsay, R.; Berndt, W.; Bradshaw, A. M.; Baddeley, C.; Lee, A. F.; Lambert, R. M.; Woodruff, D. P. *Surf. Sci.* **1998**, *406* (1–3), 90–102.
- (40) Ohtani, H.; Hove, M. A. V.; Somorjai, G. A. *Surf. Sci.* **1987**, *187* (2–3), 372–386.
- (41) Xue, L. Q.; Pang, X. Y.; Wang, G. C. *J. Phys. Chem. C* **2007**, *111* (5), 2223–2228.
- (42) Alfonso, D. R. *Surf. Sci.* **2005**, *596* (1–3), 229–241.
- (43) Gajdos, M.; Eichler, A.; Hafner, J. *J. Phys.: Condens. Matter* **2004**, *16* (8), 1141–1164.
- (44) Abild-Pedersen, F.; Andersson, M. P. *Surf. Sci.* **2007**, *601* (7), 1747–1753.
- (45) Hammer, B.; Norskov, J. K. *Surf. Sci.* **1995**, *343* (3), 211–220.
- (46) Rodriguez, J. A.; Chaturvedi, S.; Jirsak, T.; Hrbek, J. *J. Chem. Phys.* **1998**, *109* (10), 4052–4062.
- (47) Rodriguez, J. A.; Jirsak, T.; Chaturvedi, S. *J. Chem. Phys.* **1999**, *110* (6), 3138–3147.
- (48) Rodriguez, J. A.; Hrbek, J.; Kuhn, M.; Jirsak, T.; Chaturvedi, S.; Maiti, A. *J. Chem. Phys.* **2000**, *113* (24), 11284–11292.
- (49) Yang, Z. X.; Wu, R. Q.; Rodriguez, J. A. *Phys. Rev. B* **2002**, *65* (15), 155409.
- (50) Chen, L.; Chen, B.; Zhou, C.; Wu, J.; Forrey, R. C.; Cheng, H. *J. Phys. Chem. C* **2008**, *112* (36), 13937–13942.
- (51) Habermehl-Ćwirzeń, K.; Lahtinen, J. *Surf. Sci.* **2004**, *573* (2), 183–190.
- (52) Zhang, T. F.; Liu, Z. P.; Driver, S. M.; Pratt, S. J.; Jenkins, S. J.; King, D. A. *Phys. Rev. Lett.* **2005**, *95*, 266102.
- (53) Bader, R., *Atoms in Molecules: A Quantum Theory*; Oxford University Press: New York, 1990.
- (54) Blyholder, G. *J. Phys. Chem.* **1964**, *68*, 2772.
- (55) Lide, D. R., Ed. *Handbook of Chemistry and Physics*, 76th ed.; CRC Press: Boca Raton, FL, 1995.